Modelling PCB-153 in northern ecosystems across time, space, and species using the Nested Exposure Model

Ingjerd S. Krogseth,[1,2] Knut Breivik,[1,3] Sylvia Frantzen,[4] Bente M. Nilsen,[4] Sabine Eckhardt,[1] Therese H. Nøst,[5,6] Frank Wania[7]

[1]NILU, Tromsø, Norway, [2]Department of Arctic and Marine Biology, UiT – Arctic University of Norway, Tromsø, Norway, [3]Department of Chemistry, University of Oslo, Oslo, Norway, [4]Institute of Marine Research, Bergen, Norway, [5]Department of Community Medicine, UiT – Arctic University of Norway, Tromsø, Norway, [6]Department of Public Health and Nursing, NTNU – Norwegian University of Science and Technology, Trondheim, Norway, [7]Department of Physical and Environmental Science, University of Toronto Scarborough, Toronto, Canada

ELECTRONIC SUPPLEMENTARY INFORMATION

Table of Contents

S1. Biota parameterization

S1.1 Zooplankton

Previous Arctic ACC-Human models[1-3] have included three sympagic (ice-associated) size-fractionated zooplankton groups based on measurements from the Barents Sea Marginal Ice Zone in 2001.[4] Here, these groups were re-parameterized as three pelagic zooplankton groups, separated by feeding strategy, based on measurements from the coastal King's Bay in Svalbard (Norway) in 2008.[5] This was done because (i) research has shown that it is more correct to describe accumulation of contaminants in zooplankton based on feeding strategy rather than size[6, 7] and (ii) pelagic zooplankton is more ecologically important for the ecosystems in Norwegian marine areas than sympagic zooplankton, particularly as the Marginal Ice Zone retreats northwards due to climate change.

The current three zooplankton groups in the model are herbivorous, omnivorous, and carnivorous zooplankton represented by copepods, krill, and amphipods, respectively. The measured bioaccumulation factors (BAF) for these three groups are based on parallel measurements of PCBs and organochlorine pesticides in seawater and zooplankton sorted by species and feeding strategy.[5] This includes *Calanus hyperboreus, C. glacialis, and C. finmarchicus* (copepods), Euphausiids consisting mostly of *Thysanoessa inermis* (krill), and *Themisto abyssorum and Th. libellula* (amphipods).[5] Equations between BAF and the octanol-water partition coefficient (K_{OW}) for these three groups from King's Bay were incorporated into the model:[5]

Herbivores/copepods: $\log BAF = 0.37 \times log\ K_{OW} + 4.1$

Omnivores/krill: $\log BAF = 0.60 \times log\ K_{OW} + 3.2$

Predators/amphipods: $\log BAF = 0.59 \times log\ K_{OW} + 3.5$

Seasonally variable lipid content was incorporated for all three zooplankton groups (Fig S1). Lipid content of copepods and krill was derived from Falk-Petersen et al.,[8] while lipid content of amphipods was derived from Dale et al.[9] Based on this, lipid contents were assumed to range from 3% (March – April) to 20% (July – Aug) for copepods, from 3% (March – April) to 15% (Sept. – Nov.) for krill, and from 3% (March – April) to 10% (Nov. – Jan.) for amphipods.

S1.2 Fish

Here, updated parameterization of the four fish species is described. Parameters not mentioned here have been kept constant as in ACC-Human (for herring and Atlantic cod)[10] and the Expanded Arctic ACC-Human model (for capelin and polar cod).[2, 3]

The maturity distribution of polar cod was updated based on recent results from Nahrgang et al.[11] The maturity distribution of capelin was updated based on Baulier et al.[12]

A seasonal lipid content ranging from 2% (April) to 12% (Oct.) was incorporated for capelin based on Falk-Petersen et al.[8] A seasonal lipid-content ranging from 4% (April - June) to 17% (Sept. – Oct.) was incorporated for herring, derived based on measurements in Norwegian spring-spawning herring by Frantzen et al.[13] Lipid content in whole-fish and muscle was assumed identical for herring and capelin, as these species store lipids in their muscle and not in specific organs such as liver. However, polar cod and Atlantic cod use the liver as a lipid storage organ. Seasonal lipid content ranging from 6% (March) to 13% (Aug. – Sept.) was incorporated for polar cod (whole-fish) based on Aune et al.[14] For Atlantic cod, lipid content was assumed to be constant in both muscle (1%) and liver (50%), based on

measurements from the Institute of Marine Research showing negligible seasonal variation, and maintaining the constant lipid content in whole-fish Atlantic Cod (4.4%) from the ACC-Human model.[10]

The equation for absorption efficiency in the gastrointestinal tract of fish was adopted from the ACC-Human model,[10] and not from the Expanded Arctic ACC-Human model.[2, 3] Seasonal dietary composition of polar cod was kept constant as in the Expanded Arctic ACC-Human model,[2, 3] but dietary fractions of sympagic amphipods were replaced with pelagic amphipods.[15, 16] Young polar cod (< 1 year old) is assumed to eat only copepods.[1] Dietary composition of herring, capelin, and Atlantic cod, as well as ingestion rate for all species, is kept constant as in previous model versions.[2, 3, 10]

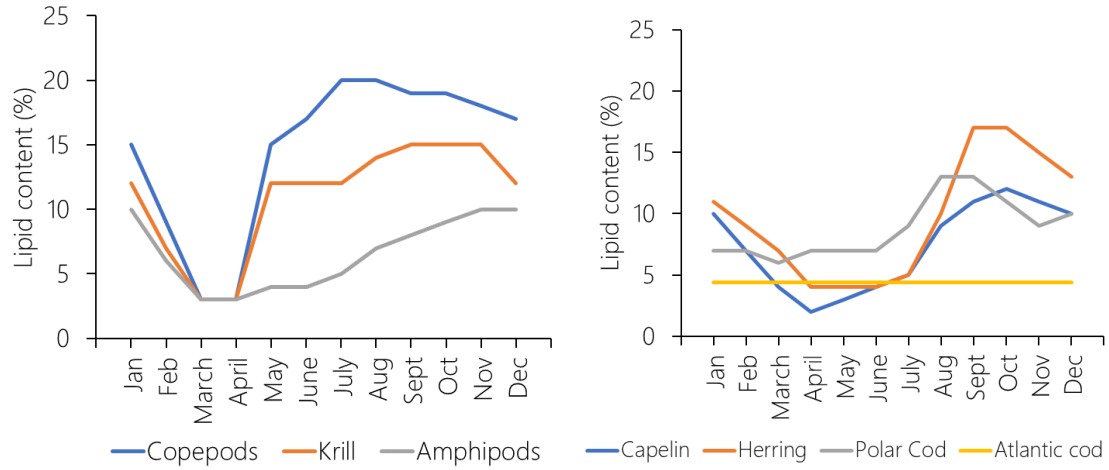

Figure S1: Seasonal lipid content in zooplankton (left) and whole-fish (right) used as model input.

S2. Maps and model domains

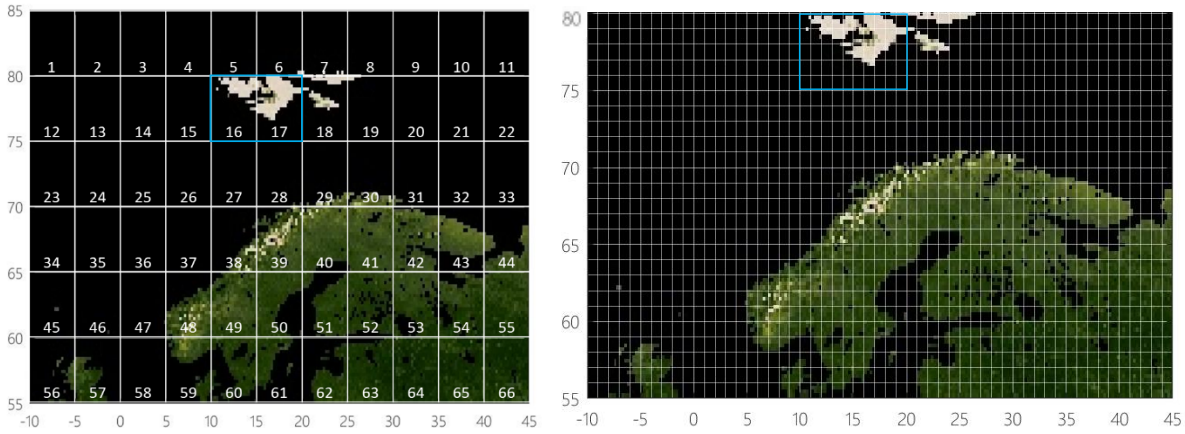

Figure S2: Illustration of the model domains for the spatial resolutions of 5° × 5° (left) and 1° × 1° (right). The blue outlines show grid cells used for simulations of Svalbard. The 5° × 5° model domain includes grid cell numbers.

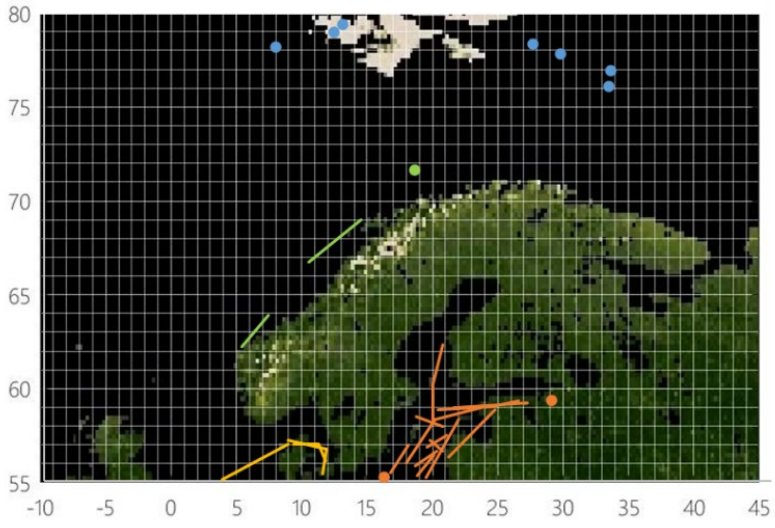

Figure S3: Location of measured seawater concentrations[5, 17-20] in the Baltic Sea (orange), North Sea and Skagerrak (yellow), Norwegian Sea (green), and Svalbard/Barents Sea region (blue) used for model evaluation. Samples collected in transects while the ship was moving are shown as lines.

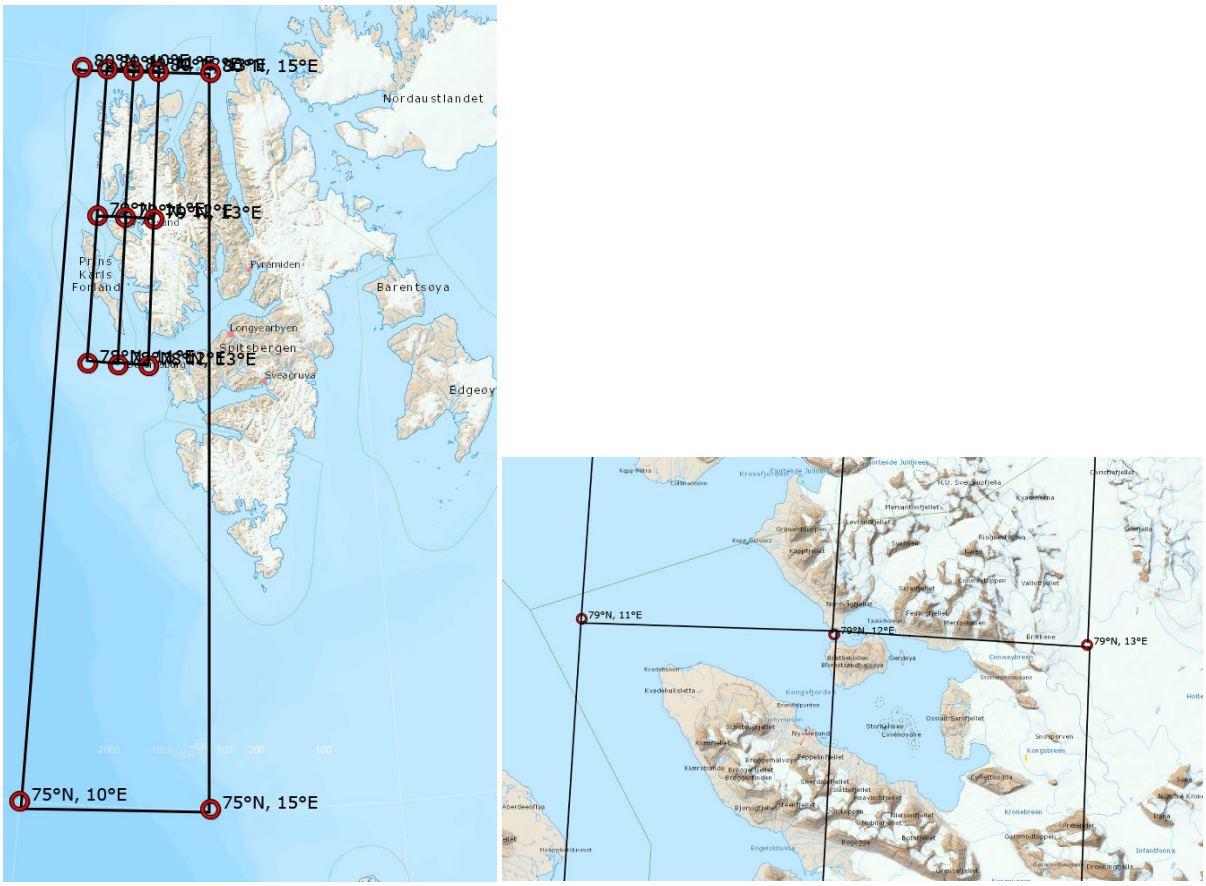

Figure S4: Map of King's Bay, Svalbard, and its alignment within the NEM model grids (5° × 5° and 1° × 1°). The right-hand map is zoomed in on King's Bay (1° × 1° grid cells only). Maps made in the Norwegian Polar Institute's topographical Svalbard map service.[21]

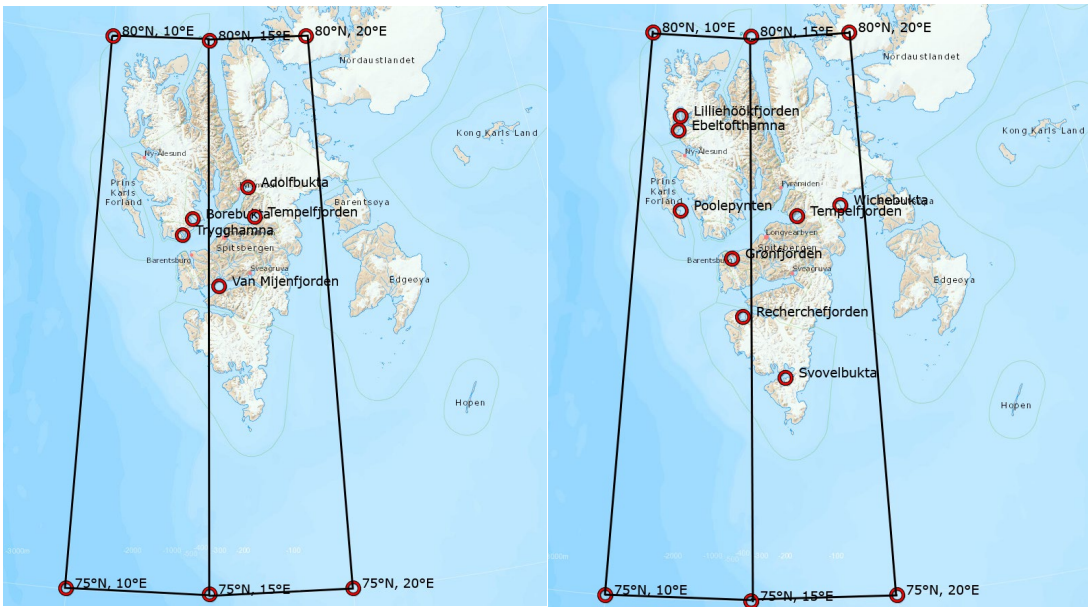

Figure S5: Approximate sampling positions for ringed seal (left) and white whale (right)[22] within the NEM model grid cells (5° × 5°). Maps made in the Norwegian Polar Institute's topographical Svalbard map service.[21]

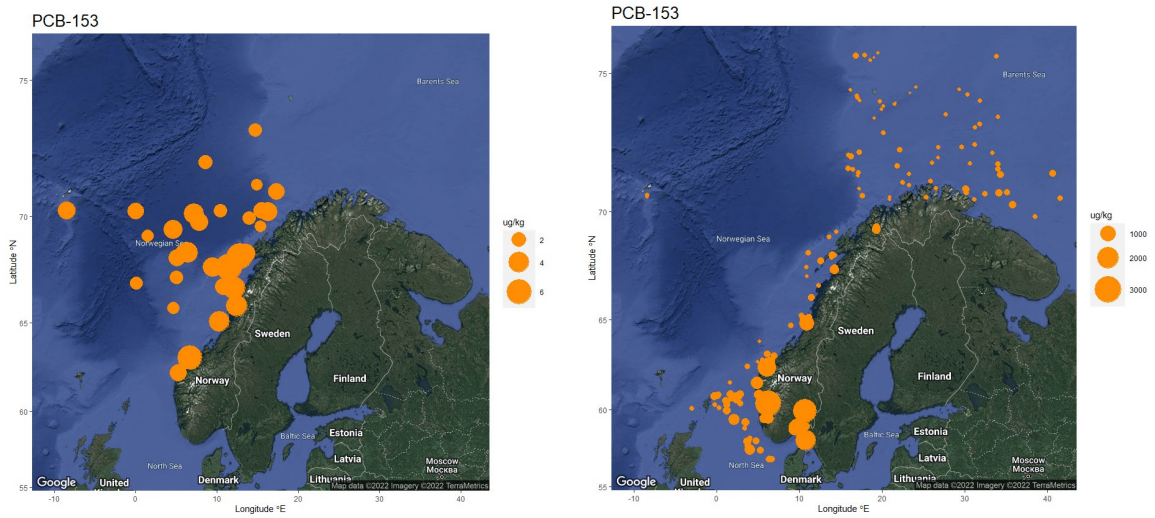

Figure S6: Measured concentrations of PCB-153 (µg/kg ww = ng/g ww) in herring muscle (left) and cod liver (right) from 2006-2018. Only samples with recorded GPS-positions are included on the map.

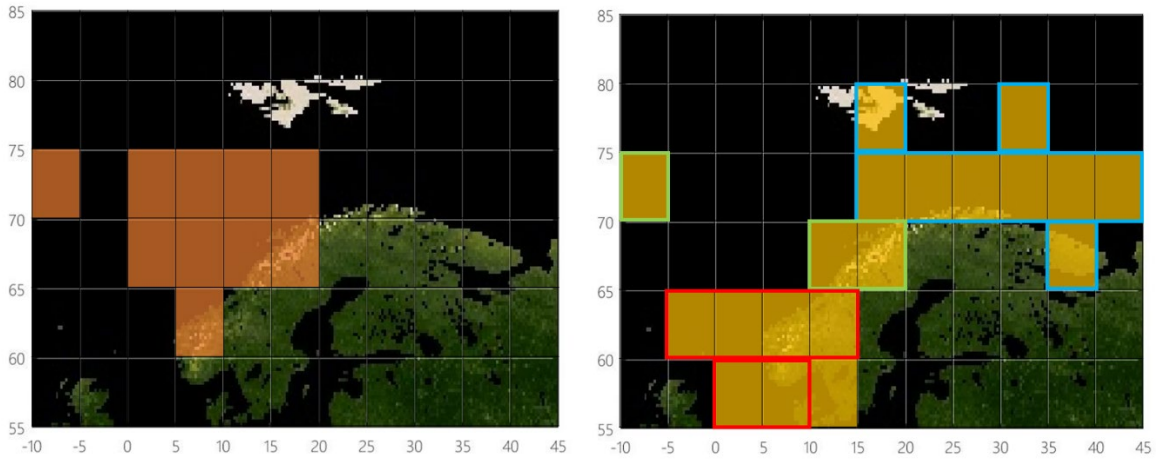

Figure S7: Illustration of grid cells (5° × 5°) with measurements of PCB-153 concentrations in herring (orange, left) and cod (yellow, right). The map for cod additionally shows which grid cells that were included in evaluation of estimated time-trends (Figure S19) for cod in the North Sea (red outline), Norwegian Sea (green outline), and Barents Sea (blue outline), respectively.

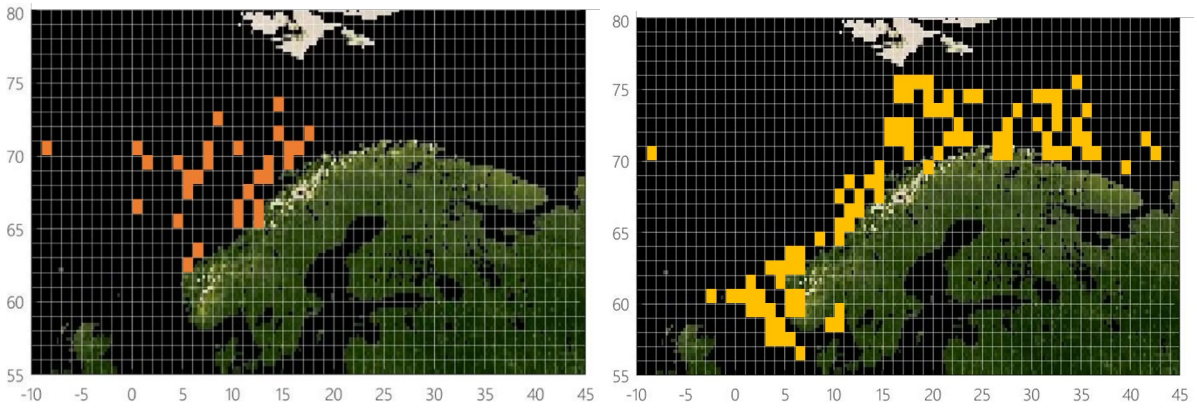

Figure S8: Illustration of grid cells (1° × 1°) with measurements of PCB-153 concentrations in herring (orange) and cod (yellow).

Table S1: Overview of number of samples with measured concentrations of PCB-153 in muscle of Norwegian spring-spawning herring and in liver of Atlantic cod, and which data selections that have been used for model evaluation.

Number of samples	Herring	Cod
Data prior to 2006	310	29
Data from 2006 onwards	944	3622
Complete dataset	1254	3651
Samples that may be impacted by local sources /elevated concentrations		144
Samples slightly impacted by local sources / elevated concentrations		113
Samples heavily impacted by local sources		229*
Dataset used for evaluation of overall time-trend	1254	3422
Samples without GPS position (prior to 2006)	310	29
Samples without GPS position (from 2006 onwards)	25	200
Dataset used for evaluation of time-trends for specific grids	919	3193
Samples without GPS, date, age and/or lipid content (after 2006)	161	1102
Dataset used for individual predictions	783	2291

**removed from dataset for model evaluation*

S4. Results for model evaluation seawater

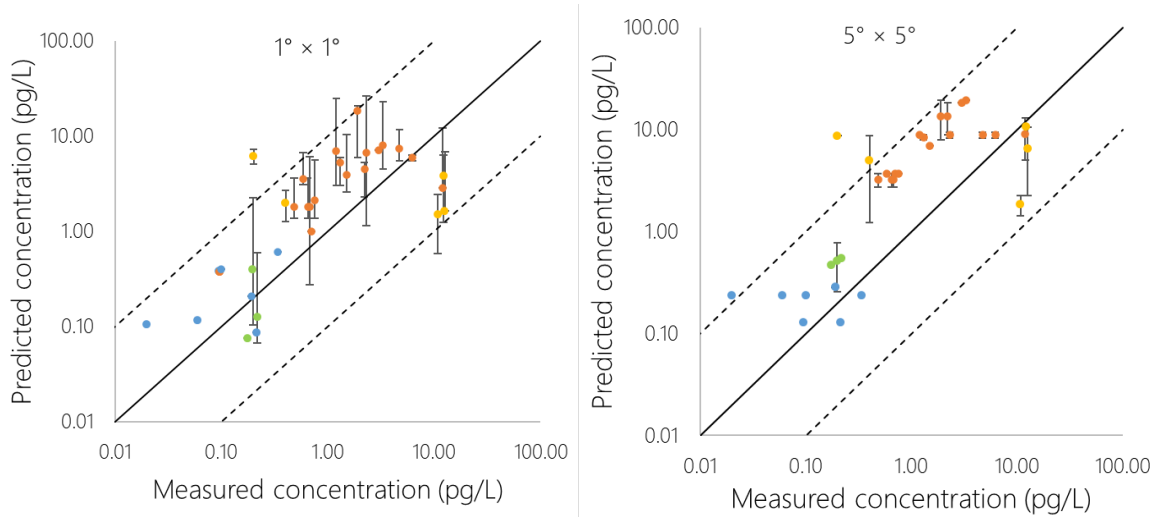

Figure S9: Results for model evaluation of dissolved PCB-153 concentrations in seawater from the Baltic Sea (orange), North Sea and Skagerrak (yellow), Norwegian Sea (green), and Barents Sea/Svalbard region (blue) (see Figure S3 for location of seawater samples). For transect samples spanning several grid cells, points and variability bars represent median and min-max of the estimated concentrations in the grid cells covering the transect. Measured concentrations are from references[5, 17-20].

S5. Results for model evaluation across species (Svalbard)

Table S2: Model evaluation for King's Bay based on the different spatial resolutions (1° × 1° and 5° × 5°). The table shows calculated PMR, model bias (MB), and $RMSE_{log}$. All total metrics (average, min, and max of PMR, as well as MB and $RMSE_{log}$) are calculated for biota only.

PMR	1° x 1°	5° x 5°
Air	0.89	1.4
Seawater	1.10	2.0
Biota		
Zooplankton	0.89	1.6
Krill	3.1	5.4
Amphipods	2.1	3.7
Capelin	1.5	2.3
Polar Cod	1.8	2.0
Atlantic cod	2.0	3.4
Ringed seal (F)	1.7	2.1
Ringed seal (M)	1.5	2.1
Beluga (F)	0.14	0.17
Beluga (M)	1.0	1.6
Average	1.6	2.4
MIN	0.14	0.17
MAX	3.1	5.4
Model bias	1.3	1.9
RMSElog	3.7	4.7

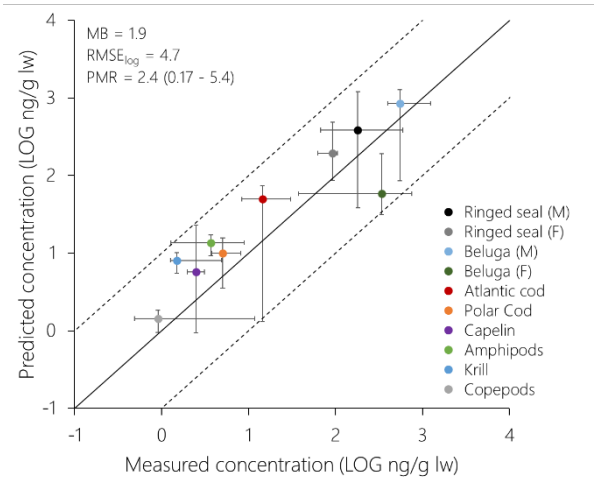

Figure S10: Model evaluation across species in King's Bay, Svalbard for PCB-153 based **on 5° × 5°** resolution. Median (point) and range (variability bars) of estimated concentrations are plotted against median (point) and range (variability bars) of measured concentrations. M = male, F = female. The solid diagonal line represents a perfect match between estimated and measured concentrations, while dashed diagonal lines show deviations of one order of magnitude.

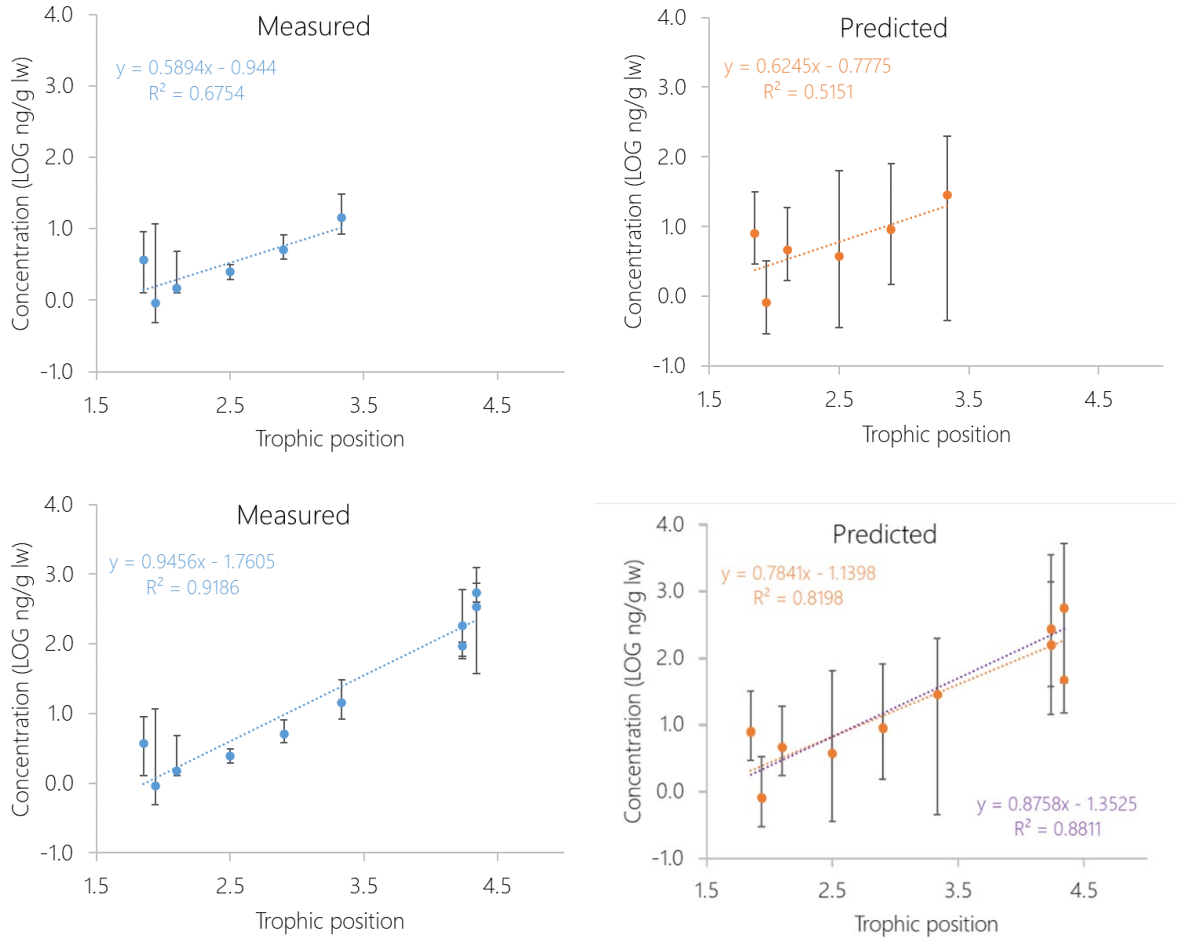

Figure S11: Measured and estimated food web magnification of PCB-153 for only poikilotherms (top) and both poikilotherms and homeotherms (bottom) based on median concentrations (and ranges) from Figure 2. Trophic positions are from Hallanger et al.[23] (poikilotherms) and calculated based on MacKenzie et al.[24] (homeotherms). The purple regression in the bottom right graph excludes female white whale.

S6. Results for model evaluation across space and time (Norwegian fish)

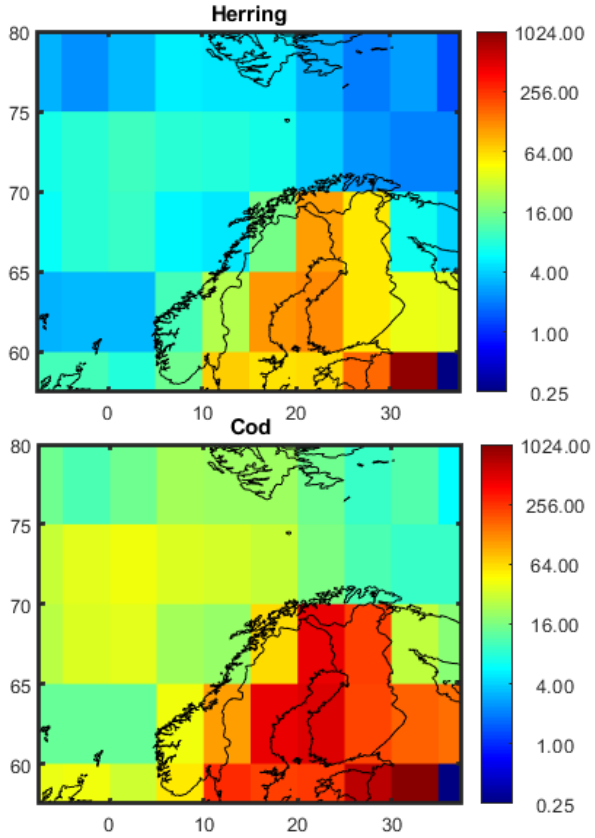

Figure S12: Maps of estimated concentrations of PCB-153 (ng/g lw) in 5-year-old herring and cod in Northern European marine areas in January 2020 based on the original 5° × 5° resolution, without the MATLAB interpolation procedure, for comparison to Figure 3.

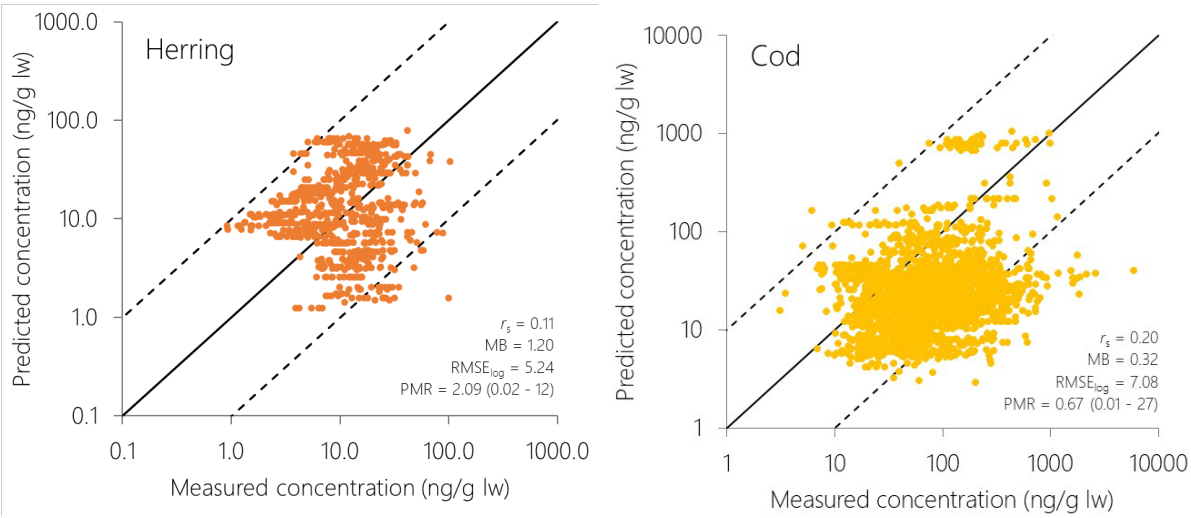

Figure S13: Model evaluation for individual estimates of PCB-153 (ng/g lw) in NSS herring and Atlantic cod in Norwegian marine areas based on a spatial resolution of **1°** × **1°**. The solid diagonal line represents a perfect match between estimated and measured concentrations, while dashed diagonal lines show deviations of one order of magnitude.

Table S3: Medians and ranges of measured and estimated concentrations for PCB-153 in herring and cod.

PCB-153 (ng/g lw)	Herring (*n* = 783)	Cod (*n* = 2291)
Measured	10.6 (0.9 - 102)	71.5 (3.1 - 5934)
Predicted (5° x 5°)	17.9 (7.3 - 109)	31.2 (6.5 - 527)
Predicted (1° x 1°)	11.1 (1.2 - 79)	23.2 (2.9 - 1031)

Table S4: Comparison of model performance for individual estimates of herring and cod based on the spatial resolutions of 5° × 5° and 1° × 1°, respectively.

	5° x 5°		1° x 1°	
	Herring	Cod	Herring	Cod
n	783	2291	783	2291
PMR average	2.87	0.78	2.09	0.67
PMR range	(0.09-19)	(0.02-21)	(0.02-12)	(0.01-27)
% within factor 4	77 %	70 %	72 %	55 %
Model bias	2.32	0.45	1.20	0.32
$RMSE_{log}$	4.71	5.66	5.24	7.08
Spearman r_s	0.65	0.22	0.11	0.20

Table S5: Comparison of model performance for individual estimates of cod from areas impacted by local sources of pollution to different extents (see Table S1) based on the spatial resolutions of 5° × 5°. Samples heavily influenced by local sources were excluded from the dataset but are included here for comparison.

5° x 5°	Not at all	Maybe	Slightly	Heavily
n	2146	96	49	25
PMR average	0.8	0.49	0.71	0.23
PMR range	(0.02-21)	(0.02-3.6)	(0.12-2.1)	(0.002-1.0)
Model bias	0.46	0.33	0.61	0.14
RMSElog	5.68	6.2	3.3	10

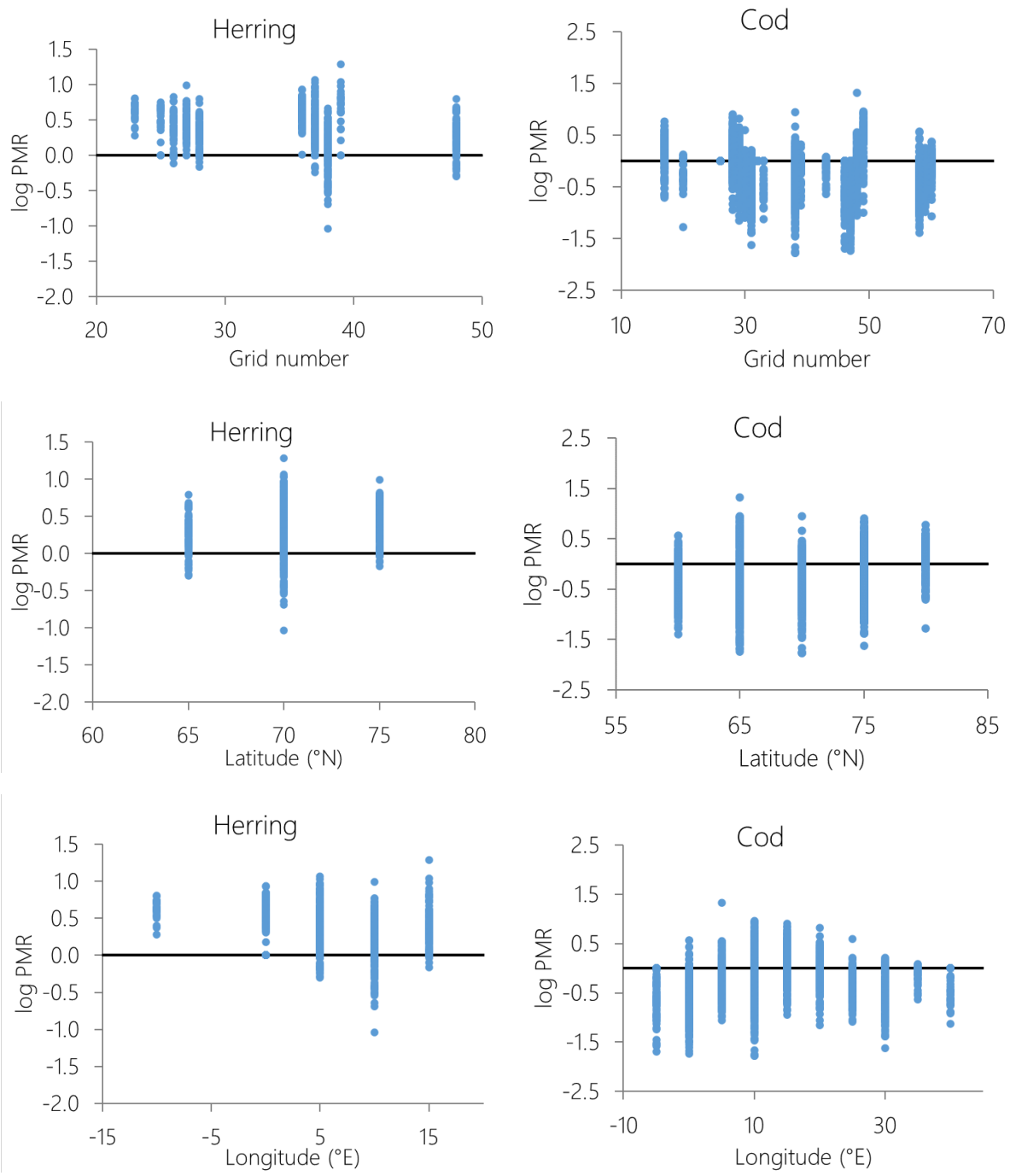

Figure S14: Logarithm of the PMR plotted against grid cell number (top), latitude (middle), and longitude (bottom) for individual estimates of herring (left) and cod (right) based on **5° × 5°** resolution. Latitude and longitude are the latitude and longitude of the northwest (NW) corner of the respective model grid cell. The black horizontal line indicates a perfect fit between model estimates and measurements (PMR = 1).

Table S6: Overview of median and ranges of measured and estimated concentrations of PCB-153 in cod liver (ng/g lw) in the four different seas/regions of the Norwegian marine areas.

PCB-153 (ng/g lw)	Skagerrak (*n* = 80)	North Sea (*n* = 775)	Norw. Sea (*n* = 527)	Barents Sea (*n* = 909)
Measured	328 (44 - 5934)	111 (7.6 - 1160)	84 (3.5 - 1881)	40 (3.1 - 486)
Predicted (5° x 5°)	294 (53 - 527)	28 (12 - 110)	45 (12 - 270)	23 (6.5 - 83)

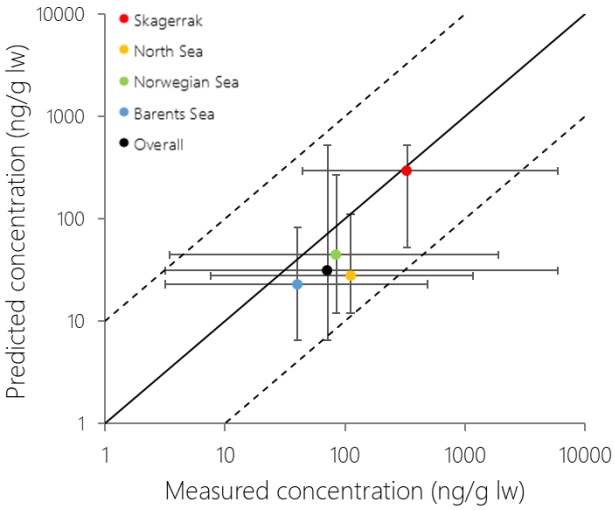

Figure S15: Model evaluation for overall estimates of PCB-153 (ng/g lw) in Atlantic cod in Skagerrak, North Sea, Norwegian Sea, and Barents Sea separately, based on a spatial resolution of **5**° × **5**°. Points and variability bars represent median and range (min-max) in concentrations, respectively. The solid diagonal line represents a perfect match between estimated and measured concentrations, while dashed diagonal lines show deviations of one order of magnitude.

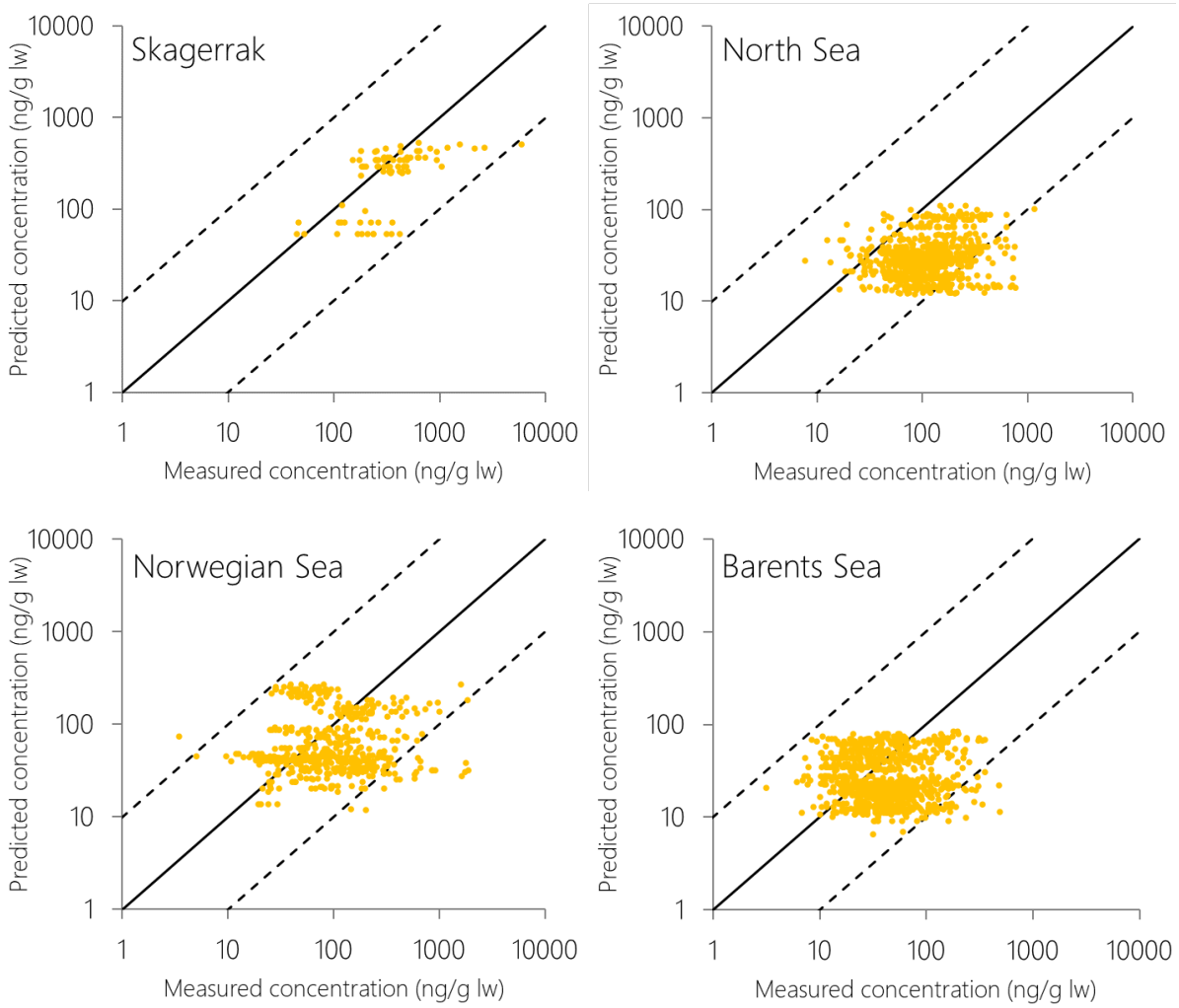

Figure S16: Model evaluation for individual estimates of PCB-153 concentrations (ng/g lw) in Atlantic cod in Skagerrak, North Sea, Norwegian Sea, and Barents Sea separately, based on a spatial resolution of **5°** × **5°**. The solid diagonal line represents a perfect match between estimated and measured concentrations, while dashed diagonal lines show deviations of one order of magnitude.

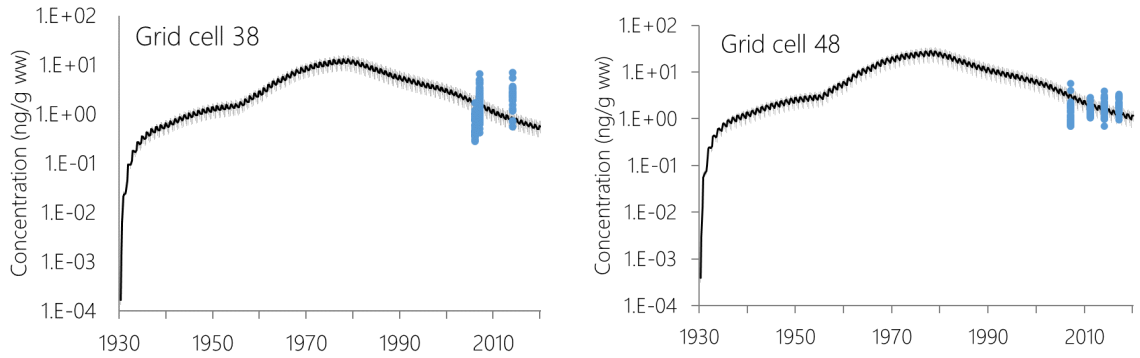

Figure S17: Estimated and measured concentrations of PCB-153 (ng/g ww) in **herring** in grid cells where measurements had been made in at least two different years (from 2006 onward when sampling positions in lat/long were available): Cells 38 (65-70°N 10-15°E) and 48 (60-65°N 5-10°E). The black line and the grey area represent the median and range of estimates, respectively. Blue markers represent measurements of PCB-153 in fish sampled within the given cell. Only measurements with GPS positions are included (i.e. only data from 2006 onwards).

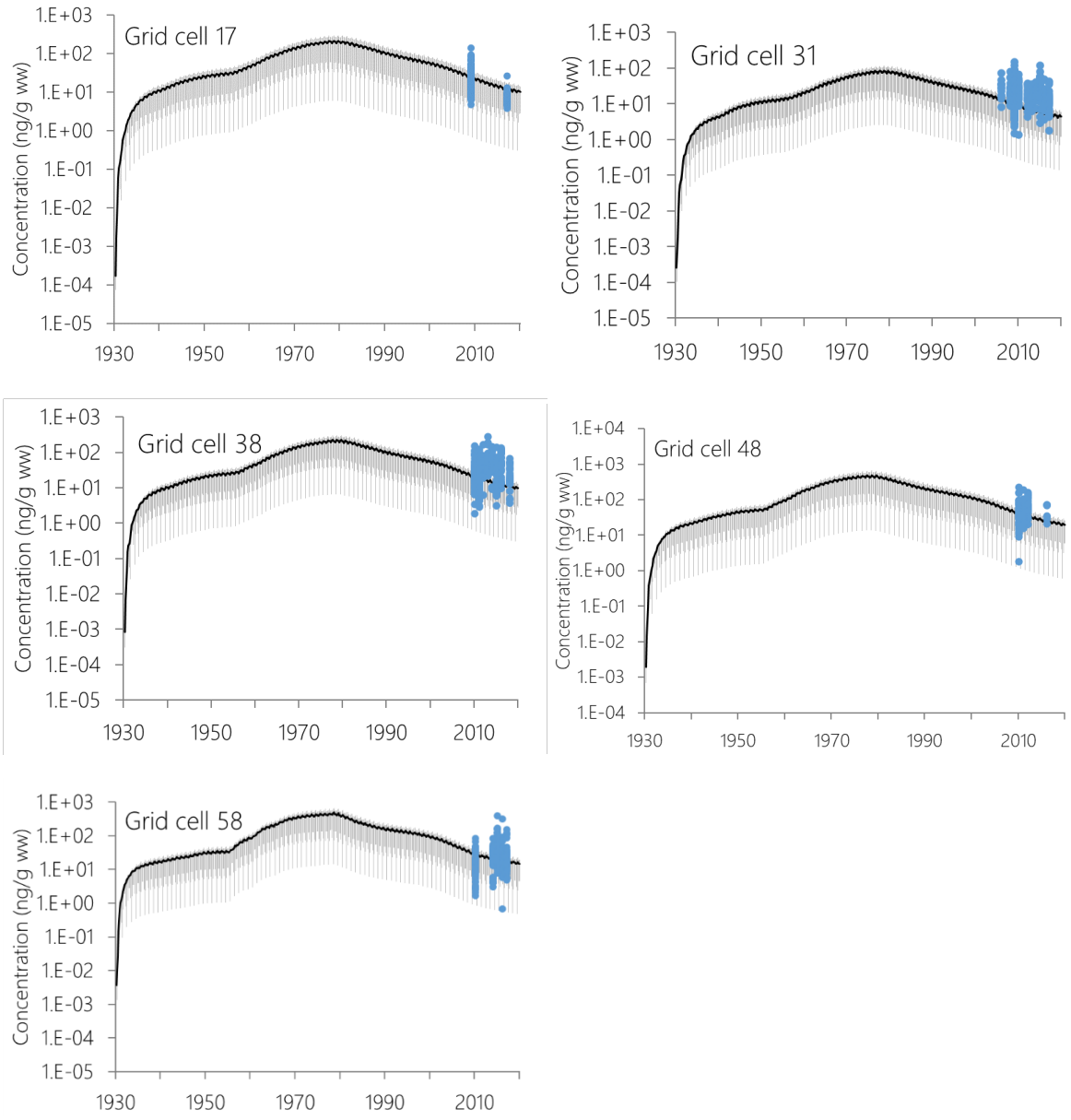

Figure S18: Estimated and measured concentrations of PCB-153 (ng/g ww) in **cod** in grid cells where measurements had been made in at least two different years (from 2006 onward when sampling positions in lat/long were available): Cells 17 (75-80°N 15-20°E), 31 (70-75°N 30-35°E), 38 (65-70°N 10-15°E), 48 (60-65°N 5-10°E), 58 (55-60°N 0-5°E) (see Figure S2 for location of grid cells). The black line and the grey area represent the median and range of estimates, respectively. Blue markers represent measurements of PCB-153 in fish sampled within the given grid cell. Only measurements with GPS positions are included (i.e. only data from 2006 onwards).

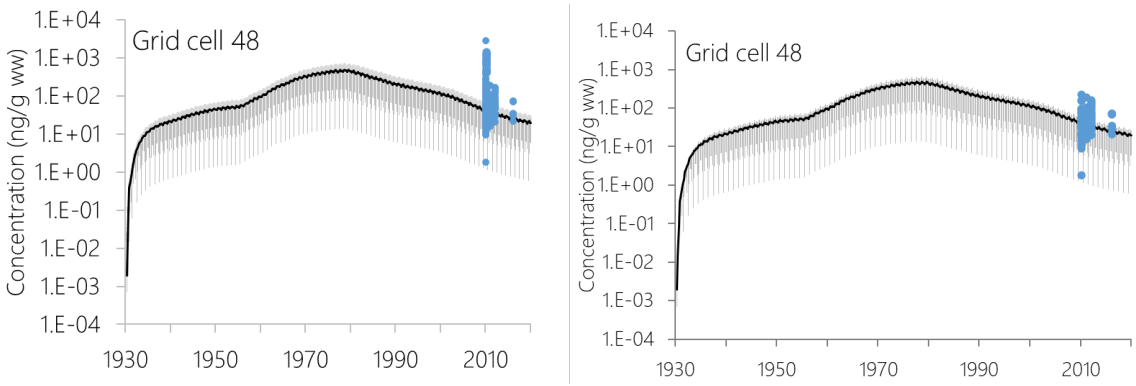

Figure S19: Estimated and measured concentrations of PCB-153 (ng/g ww) in cod in grid cell 48 with (left) and without (right) measurements flagged as heavily impacted by local sources (Table S1). The right graph is the same graph as in Figure S17.

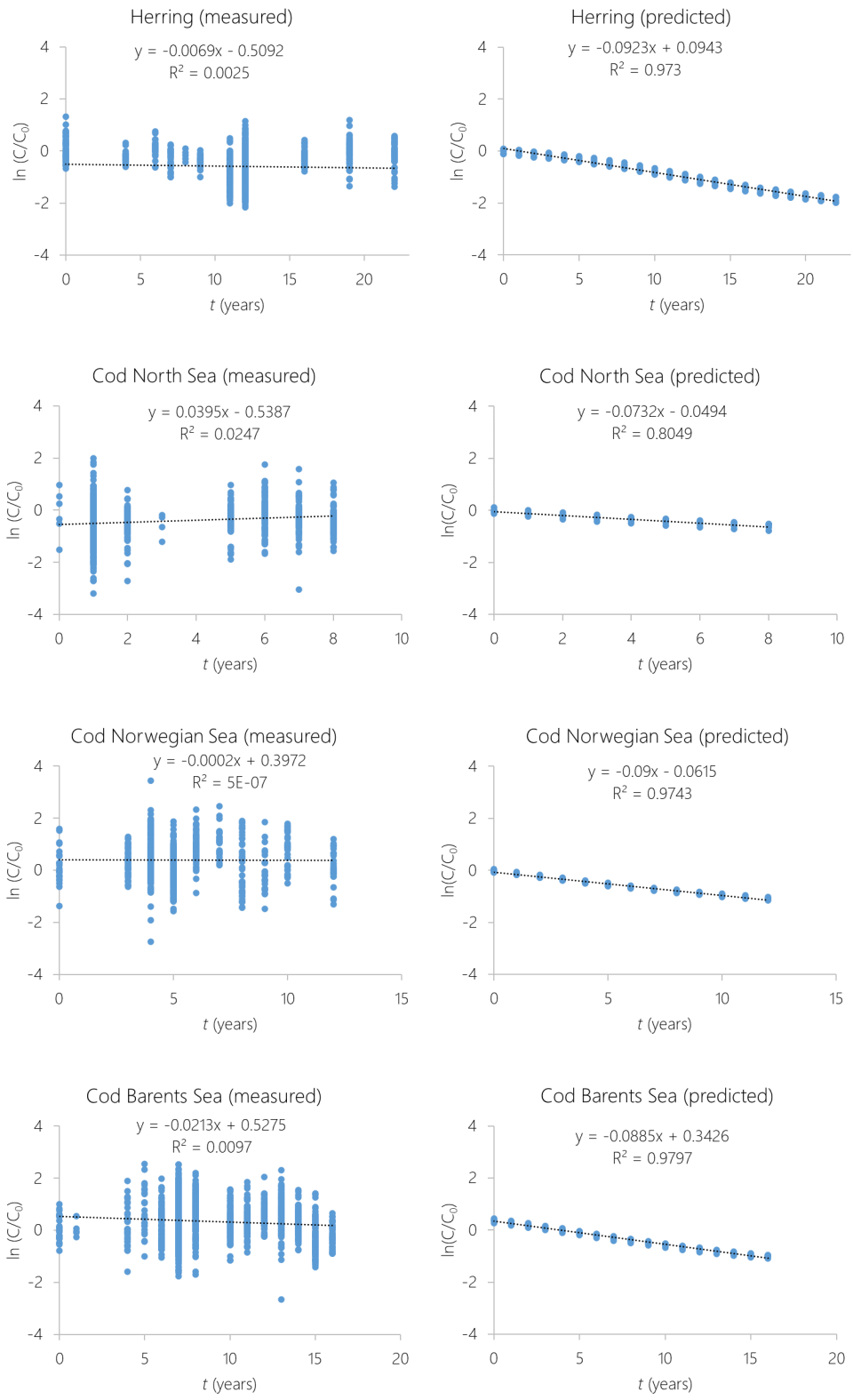

Figure S20: Linear regression to derive environmental half-lives for PCB-153 concentrations in herring and cod. For estimated concentrations, only medians across grids and age of the fish are included. The time (t) in years indicates elapsed time since the start time (t_0) of the measured time series (herring: 1995-2017, cod North Sea: 2009-2017, cod Norwegian Sea: 2006-2018, cod Barents Sea: 2002-2018).

Table S7: Linear regression to derive environmental half-lives ($t_{1/2}$) for PCB-153 concentrations in herring and cod. Numbers in bold are significant on a 95% confidence level. Numbers in green show declining concentrations with time, while numbers in red show increasing concentrations with time with a negative $t_{1/2}$ which is a doubling time rather than a half-life.

			Measurements				Predictions			
Species	Sea region	Time period	*n* (fish)	*k* (year-1)	*t1/2* (years)	*p* -value	n (grid cells)	*k* (year-1)	*t1/2* (years)	*p* -value
Herring	Norwegian Sea	1995 - 2017	1099	6.9E-03	100	9.49E-02	10	**9.2E-02**	**7.5**	**1.72E-90**
Cod	North Sea	2009 - 2017	1026	**-3.9E-02**	**-17.6**	**4.27E-07**	6	**7.3E-02**	**9.5**	**7.36E-17**
Cod	Norwegian Sea	2006 - 2018	688	2.3E-04	3071	9.86E-01	3	**9.0E-02**	**7.7**	**8.60E-52**
Cod	Barents Sea	2006 - 2018	1556	**2.1E-02**	**32.6**	**8.93E-05**	9	**8.8E-02**	**7.8**	**5.56E-72**

S7. Results for emission scenarios

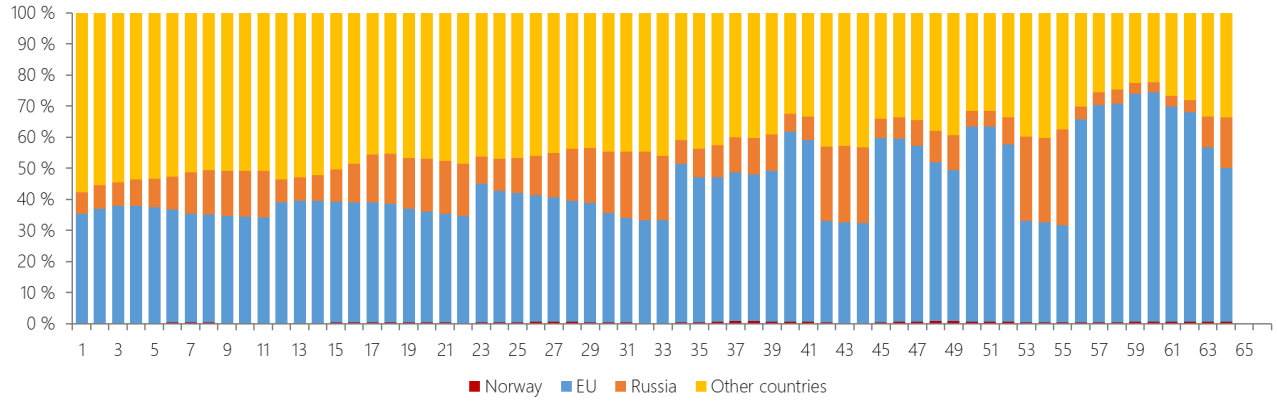

Figure S21: Contribution of primary emissions originating from Norway, EU (member countries as of 1973), Russia, and all other countries to the total body burden of PCB-153 in Atlantic herring muscle in 2020 for all grid cells (see Figure S2 for location of grid cells).

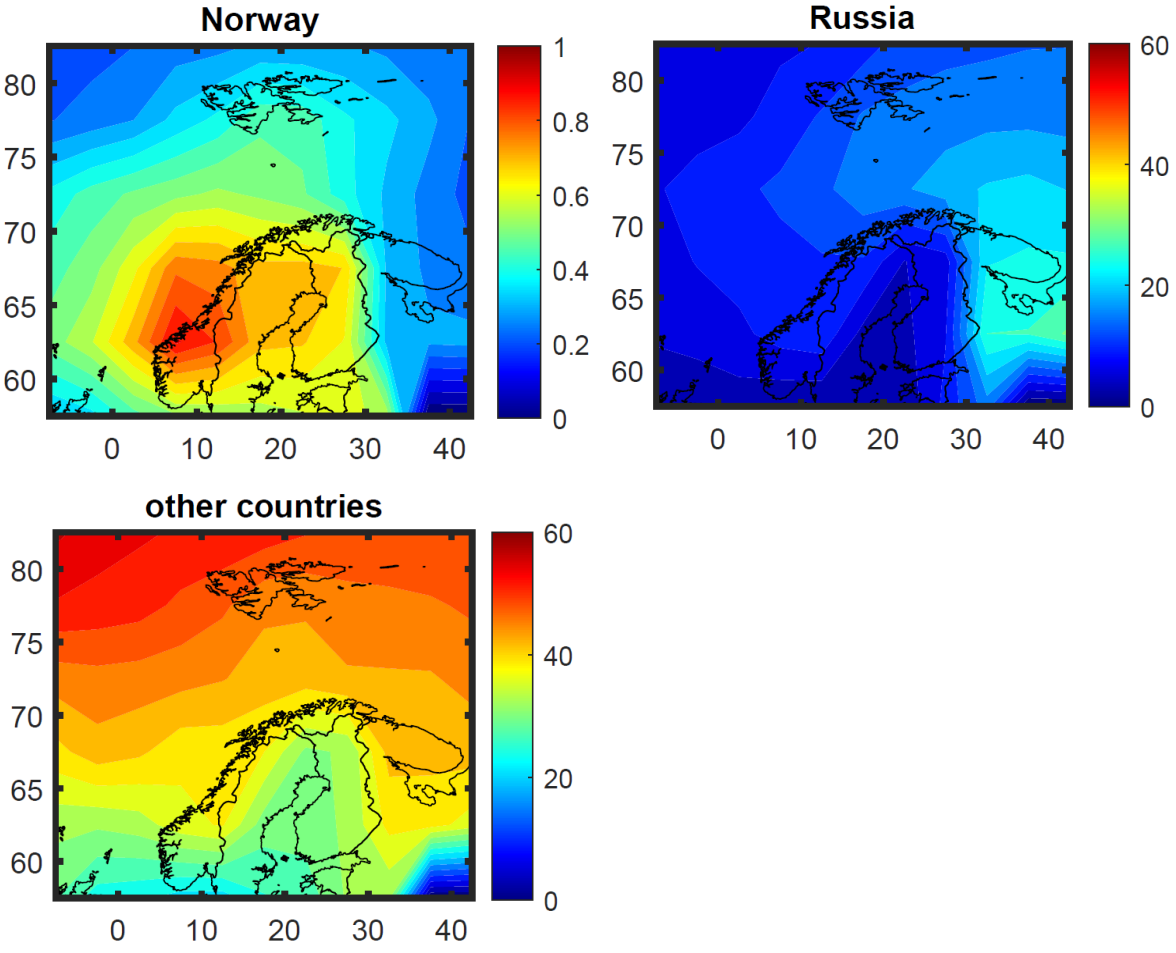

Figure S22: Fraction (in percent (%)) of total estimated PCB-153 concentrations in herring muscle in January 2020 estimated to originate from historical or ongoing primary emissions in Norway, Russia, and "other countries" (i.e. from all countries except Norway, Russia, and EU member states as of 1973). Note the different color scale in the map for Norway compared to the other maps. The data has been interpolated with the MATLAB 2023a provided script contourf, to give a better impression of the spatial distribution (see Figure 3 and Figure S12).

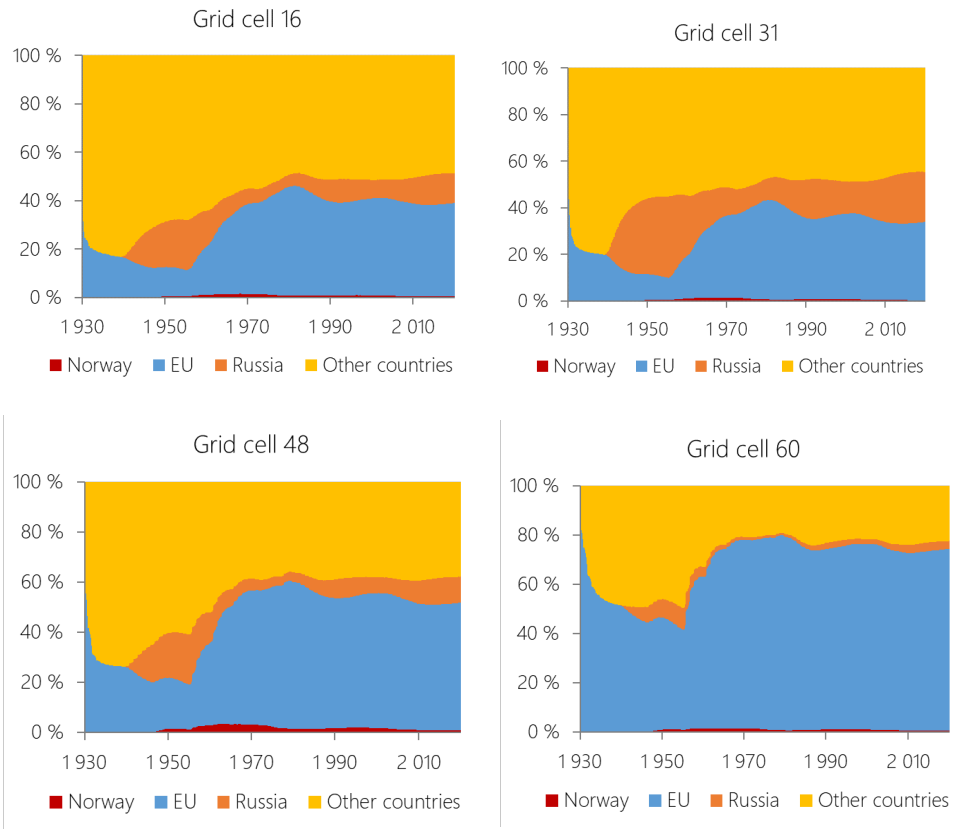

Figure S23: Temporal variation in the contribution of historical and ongoing primary emissions originating from Norway, EU (member countries as of 1973), Russia, and other countries to the total body burden of PCB-153 in Atlantic herring muscle for the time period 1930 – 2020 for four selected grid cells (see Figure S2 for location of grid cells).

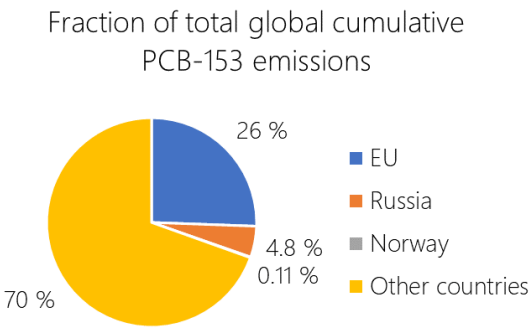

Figure S24: Fraction of total global cumulative PCB-153 emissions for the period 1930 – 2020 for Norway, EU (member countries as of 1973), Russia and other countries.

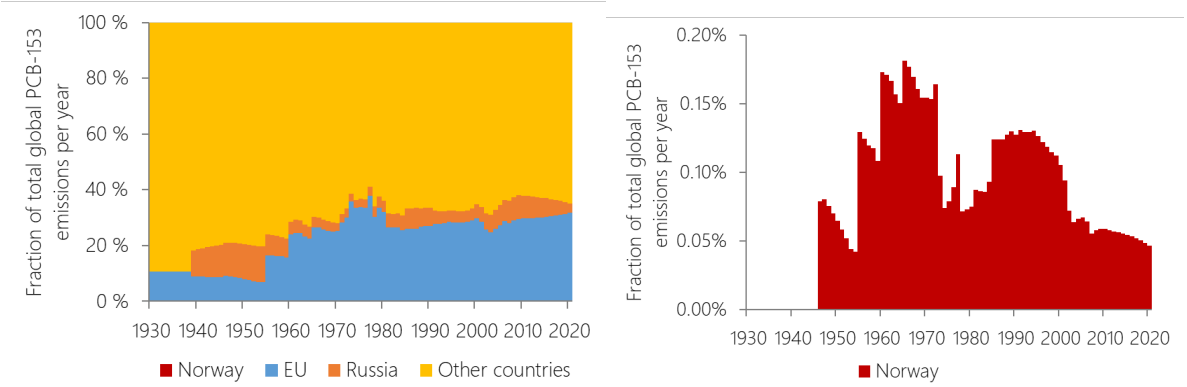

Figure S25: Fraction of total global PCB-153 emissions per year for Norway, EU (member countries as of 1973), Russia and other countries. The Norwegian fraction is also shown in a separate graph (right) as it is not visible in the left graph due to the small relative size of Norwegian emissions.

S8. Exploration of migration scenarios

Method

One of the main limitations of the current version of the NEM bioaccumulation module is that it does not account for movement of biota between grid cells. Hence, two simplified seasonal migration scenarios were explored for NSS herring and Northeast Atlantic cod to evaluate how it impacts estimated concentrations of PCB-153 as well as model performance. One scenario was constructed for each species (Figure S25): (1) NSS herring migrating seasonally between coastal (winter) and offshore (summer) areas in the Norwegian Sea. (2) Northeast Atlantic cod seasonally migrating between the Barents Sea (summer) and the Lofoten region in northern Norway (winter). Seawater fugacities and temperatures from the respective grid cells were used as input for the times of year when the fish are assumed to reside within these cells. This was used as input to estimate PCB-153 concentrations in herring or cod assumed to undergo the same migration route every year for their whole life. These simplified scenarios have two main limitations: (1) They do not account for variation in migration strategies with age or size of the fish and between individuals. (2) They assume that prey species undertake the same spatial migration as the herring or cod. This does not matter for herring, as zooplankton is anyway assumed to be in equilibrium with the surrounding seawater. However, it matters for cod as it implies that the herring consumed by cod is also assumed to migrate between the Barents Sea and Lofoten areas, which is generally not the case.

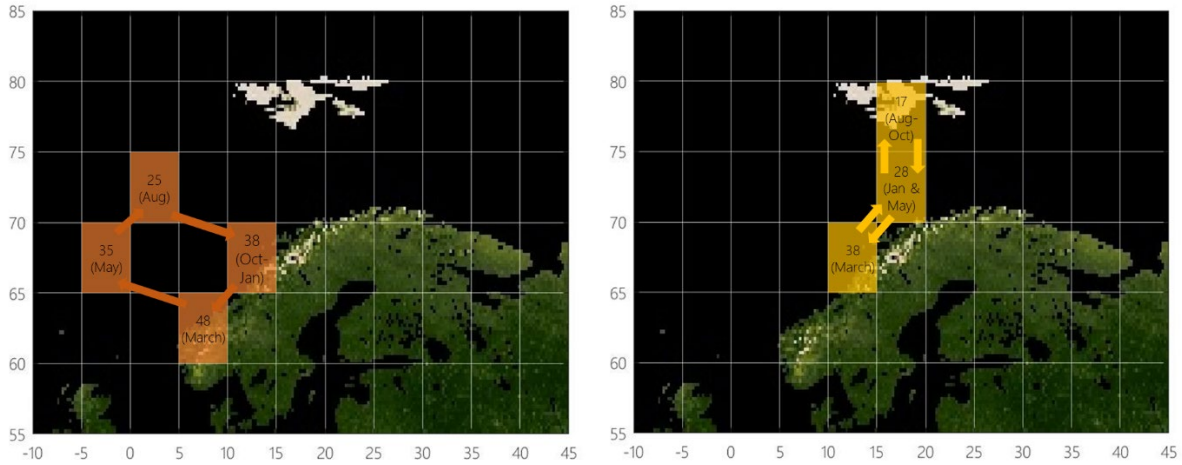

Figure S26: Illustration of the constructed seasonal migration scenarios for NSS herring (left) and Northeast Atlantic cod (right) (5° × 5° resolution). Text in grid cells indicate grid cell numbers and approximate time when they are assumed to reside within each cell. Between these time-points, the model extrapolates linearly the PCB-153 concentrations in seawater according to their migration route (indicated by arrows).

Results

In the NSS herring migration scenario, the median estimated PCB-153 concentration in herring, exemplified for 2010, was 17.8 (range 9.7 – 35.9) ng/g lw including variation with age and season. Likewise, median estimated PCB-153 concentration in cod liver, exemplified for 2010, based on the Northeast Atlantic cod migration scenario was 45.8 (range 42.8 – 48.6) ng/g lw including variation with age and season. For both herring and cod, this is basically a weighted average of the estimated concentrations in the individual grid cells in the default scenario – when the fish does not move between cells (Figure S26).

Moreover, we compared model performance for NSS herring – with and without migration – for the individual fish that had been caught along our migration route (n = 298) (i.e. in one of the four cells in Figure S25). Model performance did not improve for these fish when we included migration (Figure S27, Table S8). Both PMR, MB, $RMSE_{log}$ and Spearman r_s were comparable, but slightly poorer, in the NSS herring migration scenario compared to the default scenario (Table S8).

Model performance did not improve for cod either when we included migration (Figure S27, Table S8). In fact, for the cod caught in one of the three cells included in our migration scenario (n = 555), there is a large variation in measured concentrations that NEM is not able to capture. While the measurements span across three - four orders of magnitude, estimates range within one order of magnitude. The range in estimates is smallest when migration is included, as all estimates are based on the same migration route, and only include variation with sampling time and age of the fish (and not sampling location). As discussed previously, empirical variability in diets, ecology etc. might be significant for the cod and is currently not adequately represented in NEM.

Overall, our migration scenarios improved estimations for neither herring nor cod compared to our default scenario. However, this does not mean that spatial movement of herring and cod does not impact their contaminant concentrations. First, our migration scenarios were very simplified compared to reality. Also, using a finer spatial resolution in NEM may be required when running migration scenarios, as the coarse resolution currently applied (5° × 5°) may not capture the spatial trends in PCB-153 concentrations observed within their migration route well enough. Moreover, the cod migration scenario assumes that its prey (the herring) migrates the same route, which is not the case. Implementing different spatial movements for different species in NEM is required to enable assessment of spatial migrations more precisely. However, as the evaluation for Northeast Atlantic cod shows (Figure S27) there may be other factors impacting the variation in observed concentrations, e.g., variation in diets and/or ecology, that may be more important to include than migration.

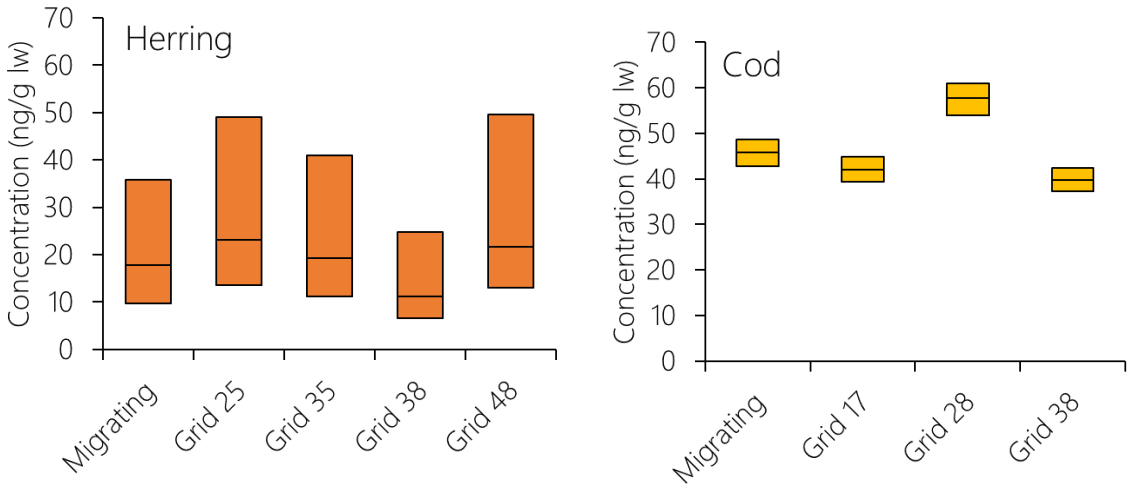

Figure S27: Median and range of estimated PCB-153 concentrations (ng/g lw) in herring muscle and cod liver exemplified for 2010, including variability with age and season. Results are included for the migration scenarios, as well as for the individual grid cells in the default scenario for comparison.

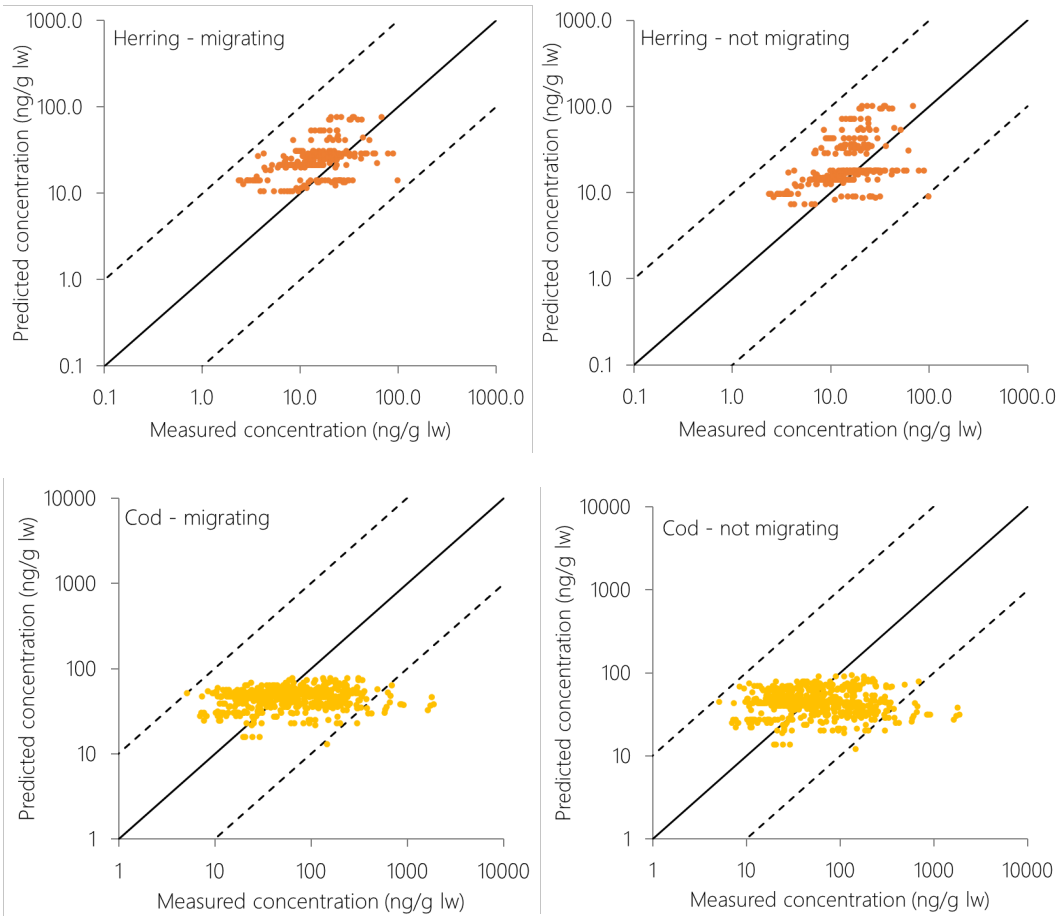

Figure S28: Model evaluation for estimates of PCB-153 for migrating herring and cod (left) compared to the default scenario where fish remain within their respective grid cells for their whole life (right). Results are only included for fish caught within the grid cells included in the explored migration scenarios (Figure S25).

Table S8: Comparison of model performance for the migration scenarios and for the default scenario where migration is not included.

	Migrating		Not migrating	
	Herring	Cod	Herring	Cod
n	298	555	298	555
PMR average	2.1	1.3	1.8	1.3
PMR range	(0.1-7.4)	(0.02-10)	(0.1-6.3)	(0.02-9)
% within factor 4	92 %	82 %	91 %	80 %
Model bias	1.8	0.8	1.5	0.8
RMSElog	3.6	4.7	3.3	4.9
Spearman r_s	0.48	0.11	0.55	-0.01

References

1. G. Czub, F. Wania and M. S. McLachlan, Combining long-range transport and bioaccumulation considerations to identify potential Arctic contaminants, *Environ. Sci. Technol.*, 2008, **42**, 3704-3709, DOI: 10.1021/es7028679.
2. M. J. Binnington and F. Wania, Clarifying relationships between persistent organic pollutant concentrations and age in wildlife biomonitoring: Individuals, cross-sections, and the roles of lifespan and sex *Environ. Toxicol. Chem.*, 2014, **33**, 1415-1426, DOI: 10.1002/etc.2576.
3. M. J. Binnington, M. S. Curren, C. L. Quinn, J. M. Armitage, J. A. Arnot, H. M. Chan and F. Wania, Mechanistic polychlorinated biphenyl exposure modeling of mothers in the Canadian Arctic: the challenge of reliably establishing dietary composition, *Environ. Int.*, 2016, **92-93**, 256-268, DOI: 10.1016/j.envint.2016.04.011.
4. A. Sobek, M. Reigstad and Ö. Gustafsson, Partitioning of polychlorinated biphenyls between arctic seawater and size-fractionated zooplankton, *Environ. Toxicol. Chem.*, 2006, **25**, 1720-1728, DOI: 10.1897/05-319r1.1.
5. I. G. Hallanger, A. Ruus, N. A. Warner, D. Herzke, A. Evenset, M. Schøyen, G. W. Gabrielsen and K. Borgå, Differences between Arctic and Atlantic fjord systems on bioaccumulation of persistent organic pollutants in zooplankton from Svalbard, *Sci. Total Environ.*, 2011, **409**, 2783-2795, DOI: 10.1016/j.scitotenv.2011.03.015.
6. K. Borgå, G. W. Gabrielsen and J. U. Skaare, Differences in contamination load between pelagic and sympagic invertebrates in the Arctic marginal ice zone: influence of habitat, diet and geography, *Marine Ecology Progress Series*, 2002, **235**, 157-169, DOI: 10.3354/meps235157.
7. I. G. Hallanger, A. Ruus, D. Herzke, N. A. Warner, A. Evenset, E. S. Heimstad, G. W. Gabrielsen and K. Borgå, Influence of season, location, and feeding strategy on bioaccumulation of halogenated organic contaminants in Arctic marine zooplankton, *Environ. Toxicol. Chem.*, 2011, **30**, 77-87, DOI: 10.1002/etc.362.
8. S. Falk-Petersen, C. C. E. Hopkins and J. R. Sargent, Trophic relationships in the pelagic, Arctic food web, *Trophic Relationships in the Marine Environment: Proceedings of the 24th European Marine Biology Symposium*, 1990, 315-333.
9. K. Dale, S. Falk-Petersen, H. Hop and S. E. Fevolden, Population dynamics and body composition of the Arctic hyperiid amphipod *Themisto libellula* in Svalbard fjords, *Polar Biol.*, 2006, **29**, 1063-1070, DOI: 10.1007/s00300-006-0150-5.
10. G. Czub and M. S. McLachlan, A food chain model to predict the levels of lipophilic organic contaminants in humans, *Environ. Toxicol. Chem.*, 2004, **23**, 2356-2366, DOI: 10.1897/03-317.

11. J. Nahrgang, Ø. Varpe, E. Korshunova, S. Murzina, I. G. Hallanger, I. Vieweg and J. Berge, Gender specific reproductive strategies of an Arctic key species (*Boreogadus saida*) and implications of climate change, *PLOS ONE*, 2014, **9**, e98452, DOI: 10.1371/journal.pone.0098452.
12. L. Baulier, M. Heino and H. Gjøsæter, Temporal stability of the maturation schedule of capelin *Mallotus villosus* in the Barents Sea, *Aquatic Living Resources*, 2012, **25**, 151-161, DOI: 10.1051/alr/2012014.
13. S. Frantzen, A. Måge, S. A. Iversen and K. Julshamn, Seasonal variation in the levels of organohalogen compounds in herring (*Clupea harengus*) from the Norwegian Sea, *Chemosphere*, 2011, **85**, 179-187, DOI: 10.1016/j.chemosphere.2011.06.034.
14. M. Aune, E. Raskhozheva, H. Andrade, S. Augustine, A. Bambulyak, L. Camus, J. Carroll, A. V. Dolgov, H. Hop, D. Moiseev, P. E. Renaud and Ø. Varpe, Distribution and ecology of polar cod (*Boreogadus saida*) in the eastern Barents Sea: A review of historical literature, *Mar. Environ. Res.*, 2021, **166**, 105262, DOI: 10.1016/j.marenvres.2021.105262.
15. P. E. Renaud, J. Berge, Ø. Varpe, O. J. Lønne, J. Nahrgang, C. Ottesen and I. Hallanger, Is the poleward expansion by Atlantic cod and haddock threatening native polar cod, *Boreogadus saida*?, *Polar Biol.*, 2012, **35**, 401-412, DOI: 10.1007/s00300-011-1085-z.
16. M. L. J. Cusa, The effect of seasonality on polar cod (*Boreogadus saida*) dietary habits and temporal feeding strategies in Svalbard waters, Master thesis, UiT - The Arctic University of Norway, 2016.
17. D. E. Schulz-Bull, G. Petrick, N. Kannan and J. C. Duinker, Distribution of individual chlorobiphenyls (PCB) in solution and suspension in the Baltic Sea, *Mar. Chem.*, 1995, **48**, 245-270, DOI: 10.1016/0304-4203(94)00054-H.
18. D. Wodarg, P. Kömp and M. S. McLachlan, A baseline study of polychlorinated biphenyl and hexachlorobenzene concentrations in the western Baltic Sea and Baltic Proper, *Mar. Chem.*, 2004, **87**, 23-36, DOI: 10.1016/j.marchem.2003.12.002.
19. A. Sobek and Ö. Gustafsson, Latitudinal fractionation of polychlorinated biphenyls in surface seawater along a 62° N−89° N transect from the southern Norwegian Sea to the North pole area, *Environ. Sci. Technol.*, 2004, **38**, 2746-2751, DOI: 10.1021/es0353816.
20. K. Borgå and A. Di Guardo, Comparing measured and predicted PCB concentrations in Arctic seawater and marine biota, *Sci. Total Environ.*, 2005, **342**, 281-300, DOI: 10.1016/j.scitotenv.2004.12.043.
21. Norwegian Polar Institute, Toposvalbard, https://toposvalbard.npolar.no, (accessed 30th Sept 2021).
22. P. Blévin, J. Aars, C. Andvik, M. Biuw, K. Borgå, J. Bytingsvik, A. Fisk, T. Haug, D. Herzke, J. L. Lyche, C. Lydersen, K. Kovacs, A. Rikardsen, E. Vogel and H. Routti, Getting the full picture: Persistent organic pollutants in marine mammals from the Norwegian Arctic, In preparation.
23. I. G. Hallanger, N. A. Warner, A. Ruus, A. Evenset, G. Christensen, D. Herzke, G. W. Gabrielsen and K. Borgå, Seasonality in contaminant accumulation in Arctic marine pelagic food webs using trophic magnification factor as a measure of bioaccumulation, *Environ. Toxicol. Chem.*, 2011, **30**, 1026-1035, DOI: 10.1002/etc.488.
24. K. M. MacKenzie, C. Lydersen, T. Haug, H. Routti, J. Aars, C. M. Andvik, K. Borgå, A. T. Fisk, S. Meier, M. Biuw, A. D. Lowther, U. Lindstrøm and K. M. Kovacs, Niches of marine mammals in the European Arctic, *Ecological Indicators*, 2022, **136**, 108661, DOI: 10.1016/j.ecolind.2022.108661.